

GPS-GLASS: Learning Nighttime Semantic Segmentation Using Daytime Video and GPS data

Hongjae Lee, Changwoo Han, and Seung-Won Jung, *Senior Member, IEEE*

Abstract—Semantic segmentation for autonomous driving should be robust against various in-the-wild environments. Nighttime semantic segmentation is especially challenging due to a lack of annotated nighttime images and a large domain gap from daytime images with sufficient annotation. In this paper, we propose a novel GPS-based training framework for nighttime semantic segmentation. Given GPS-aligned pairs of daytime and nighttime images, we perform cross-domain correspondence matching to obtain pixel-level pseudo supervision. Moreover, we conduct flow estimation between daytime video frames and apply GPS-based scaling to acquire another pixel-level pseudo supervision. Using these pseudo supervisions with a confidence map, we train a nighttime semantic segmentation network without any annotation from nighttime images. Experimental results demonstrate the effectiveness of the proposed method on several nighttime semantic segmentation datasets. Our source code is available at <https://github.com/jimmy9704/GPS-GLASS>.

Index Terms—Correspondence matching, global positioning system, nighttime image, optical flow, semantic segmentation, unsupervised domain adaptation

I. INTRODUCTION

SEMANTIC segmentation, which classifies each pixel of an image into a semantic class, is a fundamental problem in computer vision and has been widely used in various applications, including autonomous driving, robotic navigation, and medical imaging. In particular, for autonomous driving applications, it is necessary to design a segmentation method that is robust against domain changes such as illumination and weather changes. In order to design such a method, especially with convolutional neural networks (CNNs), a large amount of pixel-level annotated data is required for supervised learning. However, acquiring pixel-level annotation in poor illumination environments such as nighttime is very challenging beyond the cost of annotations. Therefore, most semantic segmentation datasets focus primarily on daytime environments [1], [2], but a semantic segmentation model trained on such datasets fails in nighttime semantic segmentation, as shown in Fig. 1. Although some datasets [3], [4] provide nighttime image annotations, their quantity and quality are insufficient to be used for semantic segmentation network training. In this paper, we propose a training methodology for nighttime image semantic segmentation networks without requiring pixel-level annotation of nighttime scenes.

Several methods have been developed to adapt daytime segmentation networks to nighttime scenes without using

Corresponding author: Seung-Won Jung.

The authors are with the Department of Electrical and Electronic Engineering, Korea University, Seoul, Korea. (e-mail: jimmy9704@korea.ac.kr; hcwoo329@korea.ac.kr; swjung83@korea.ac.kr)

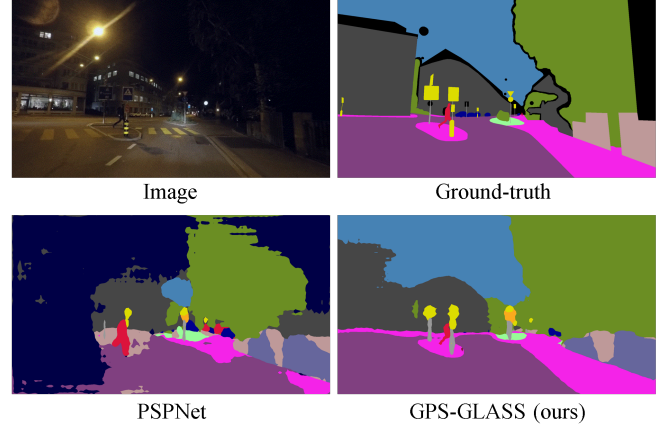


Fig. 1. Visual comparison of the nighttime semantic segmentation results between the PSPNet [5] without domain adaptation and our proposed GPS-GLASS.

annotated nighttime images. For example, the twilight domain between daytime and nighttime has been introduced for gradual domain adaptation [3], [6], [7]. Image translation has also been attempted to obtain synthetic annotations of nighttime images that can help train semantic segmentation networks [8], [9]. However, these methods require additional training data in the twilight domain or several pre-processing stages. Several recent methods [10], [11] have presented pseudo-supervised loss terms using coarsely aligned daytime and nighttime image pairs. These recent methods require neither additional domain data nor pre-processing stages, but they have not attempted to align daytime and nighttime image pairs precisely.

In this paper, we present a novel Global Positioning System (GPS)-Guided Learning Approach for nighttime Semantic Segmentation (GPS-GLASS), as illustrated in Fig. 2. Similar to DANNet [10], GPS-GLASS uses image relighting and semantic segmentation modules and two discriminators for the daytime and nighttime domains. Unlike DANNet, GPS-GLASS extracts image features obtained during the segmentation process to estimate the correspondence from the daytime to nighttime and vice versa. Moreover, observing that night images are located between daytime image frames, GPS-GLASS applies intra-domain correspondence matching to daytime image frames and performs GPS-based flow scaling. From these inter-domain and intra-domain correspondences, we construct pseudo-labels for training a nighttime semantic segmentation network.

Our contributions are summarized as follows:

- We introduce a framework called GPS-GLASS that per-

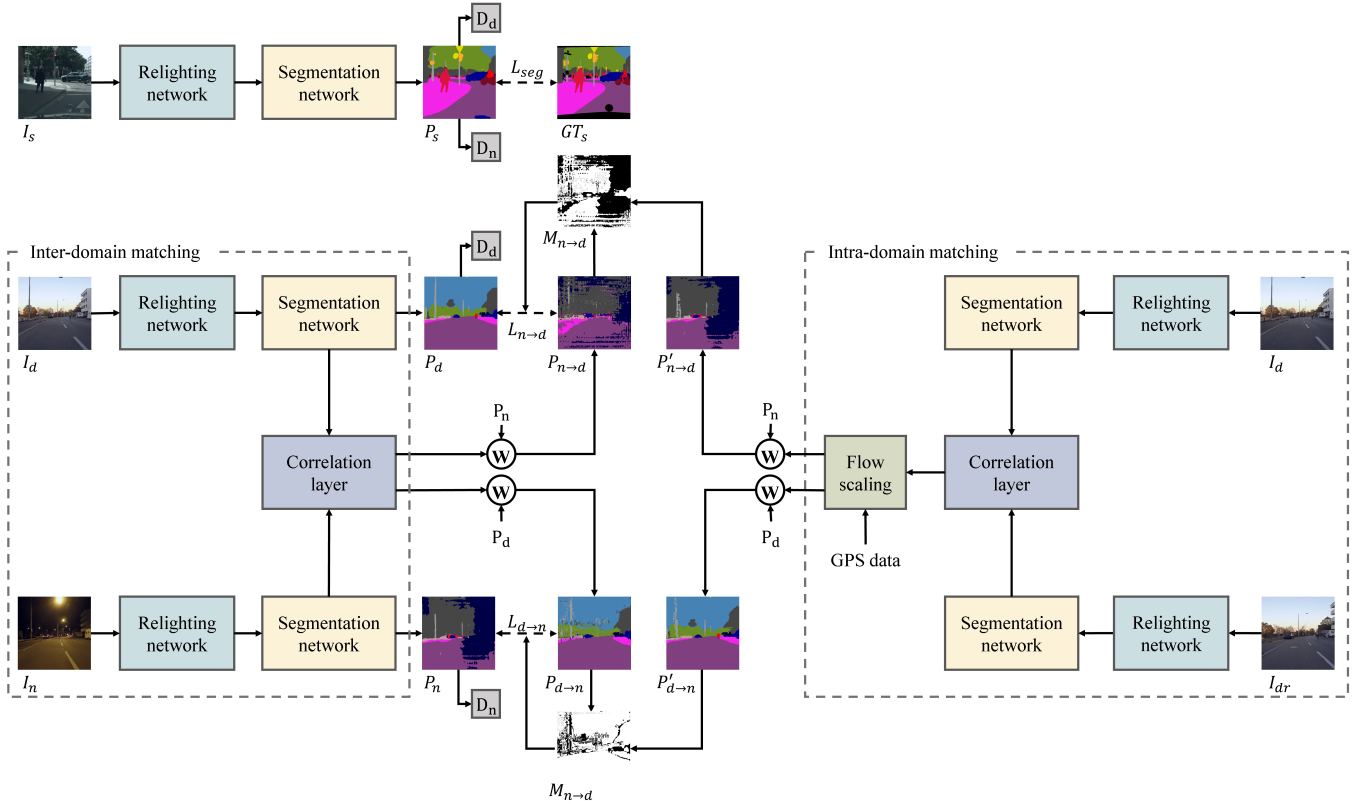


Fig. 2. The overview of the proposed GPS-GLASS. The same colored networks share weights, and the correlation layer has no weights that require training. \otimes represents the backward warping operator, and the red and blue dotted arrows indicate supervision by the ground-truth and pseudo-labels, respectively.

forms inter-domain correspondence matching to construct a pseudo-label for training a nighttime semantic segmentation network.

- We propose to perform intra-domain correspondence matching using daytime video frames and scale the estimated flow field using GPS data, yielding another pseudo-label.
- By combining the two pseudo-labels with a confidence map, GPS-GLASS shows state-of-the-art performance on several nighttime image datasets. Ablation studies also verify the effectiveness of each component of GPS-GLASS.

II. RELATED WORK

A. Unsupervised Domain Adaptation for Semantic Segmentation

Supervised training of semantic segmentation networks requires pixel-level annotation, which is laborious and time-consuming to obtain. Because ground-truth annotation is publicly available only for some limited domains, e.g., Cityscapes [1] for daytime road scenes and GTA5 [12] for synthetic scenes, unsupervised domain adaptation (UDA) has received significant interest. There have been several approaches [13], [14] to achieve the goal of UDA for semantic segmentation, i.e., reducing the domain gap between the source and target distributions without requiring annotation of the target domain.

Since the pioneering work of Ganin et al. [15], domain adversarial training has been extensively applied to semantic segmentation. Hoffman et al. [16] was the first to apply domain adversarial training to fully convolutional models for dense prediction tasks, including semantic segmentation. Du et al. [17] addressed the inconsistent adaptation issue in the traditional class-wise adversarial learning and introduced principal adaptation direction to separate features for independent adaptation operation. Tsai et al. [18] proposed to learn discriminative feature representations of image patches in the source domain and guided the target patch feature representations to be located closer to the distributions of source patches. In addition to domain adversarial training, image style transfer [19]–[21] has been investigated as a promising solution for UDA-based semantic segmentation. To this end, Lee et al. [22] focused on extracting the content information that does not suffer from the domain gap. Yang et al. [23] proposed to perform image style transfer using Fourier transform. Hoffman et al. [20] and Zhang et al. [24] further integrated domain adversarial training and image style transfer for effective domain gap reduction.

B. Nighttime Semantic Segmentation

Semantic segmentation plays an essential role in autonomous driving [25], [26]. Because the existing datasets developed for semantic segmentation of road scenes are biased toward daytime scenes [1], [2], segmentation networks trained without considering UDA tend to fail in handling nighttime

scenes. Consequently, efforts have been made to reduce the domain gap between daytime and nighttime scenes.

Motivated by the widely studied image style transfer [27]–[29], one can try translating daytime scenes to nighttime scenes. Earlier studies along this direction [8], [9] were overly interested in the auxiliary task of the image style transfer rather than the main semantic segmentation task. Sakaridis et al. [6] constructed the *Dark Zurich* dataset, which contains daytime and nighttime images that are coarsely matched with GPS information. These daytime and nighttime image pairs are helpful in guiding the semantic segmentation of nighttime scenes, resulting in many follow-up studies, including their guided curriculum model adaptation (GCMA). Sakaridis et al. [7] proposed an improved version of GCMA that uses depth and camera pose information. Wu et al. [10] proposed a multi-target domain adaptation network for nighttime semantic segmentation via adversarial learning. Xu et al. [11] proposed nighttime domain gradual self-training and patch-level prediction guidance methods.

However, the above methods [6], [7], [10], [11] have not attempted to precisely align daytime and nighttime images because such an alignment can even be a more difficult task than semantic segmentation. Xu et al. [30] aligned the daytime and nighttime images using an additional optical flow estimation network. However, the above method requires additional datasets and training stages for the optical flow estimation network. We notice that the invaluable information of GPS is obtainable when constructing datasets such as Dark Zurich. Consequently, in this paper, we propose to use the GPS information of daytime and nighttime images to guide the nighttime semantic segmentation network training.

C. Optical Flow

Learning-based approaches dominate the optical flow estimation task like other computer vision tasks [31], [32]. As a pioneering work, Dosovitskiy et al. [33] introduced two optical flow estimation CNNs: FlowNetS, which takes two concatenated images as the network input, and FlowNetC, which applies a correlation layer to the features extracted from two images. Ilg et al. [34] proposed an improved version of FlowNet, called FlowNet2.0. Specifically, they proposed to use small-sized kernels to predict the flow of small movements and stack multiple FlowNets. Ranjan et al. [35] proposed a spatial pyramid network that predicts flow in a coarse-to-fine manner. Sun et al. [36] proposed a method of warping the spatial feature pyramid and calculating the cost volume from the warped features. Teed et al. [37] proposed a recurrent unit for gradual flow refinement, demonstrating high performance with fewer network parameters. Recent transformer [38]-based optical flow models [39]–[41] further improved the optical flow estimation performance.

With the improvements in optical flow estimation techniques, efforts have been made to conduct optical flow estimation between images corresponding to different domains. For example, Zhou et al. [42] estimated optical flow to match and align two images captured under different weather conditions. Zhang et al. [43] proposed a method to train an

image translation network by warping images from different domains. Lee et al. [44], [45] introduced a model called SFNet that predicts bidirectional optical flow between different instances of the same object or scene category. Inspired by the superior performance of SFNet, we adapt it for our task of the alignment of segmentation maps.

III. PROPOSED METHODS

A. Framework Overview

Our method involves a source domain S and two target domains T_d and T_n , where S , T_d , and T_n correspond to Cityscapes (daytime) [1], Dark Zurich-D (daytime), and Dark Zurich-N (nighttime) [6] datasets in our case study, respectively. Note that only the source domain has ground-truth segmentation labels, and the two target domains are coarsely paired according to GPS locations. As shown in Fig. 2, our GPS-GLASS consists of a single weight-sharing relighting network (G_R), a single weight-sharing semantic segmentation network (G_S), and two discriminators (D_d and D_n), where we used the same architecture of DANNet [10] for these network components. Let I_s , I_n , and I_d denote image samples corresponding to S , T_d , and T_n , respectively. These images are fed to G_R to make G_S less sensitive to illumination changes [10]. The segmentation results are obtained as $P_s = G_S(G_R(I_s))$, $P_d = G_S(G_R(I_d))$, and $P_n = G_S(G_R(I_n))$. Only P_s has its corresponding ground-truth segmentation labels P_s^* , and the other two results P_d and P_n are supervised by the pseudo-label.

Specifically, the proposed training framework called GPS-GLASS obtains the pseudo-label by estimating dense correspondence between the daytime and nighttime images, where the correlation layer is applied to the intermediate features of the segmentation network. In addition, since the dense correspondence between daytime and nighttime images can be inaccurate, GPS-GLASS obtains another pseudo-label by estimating dense correspondence between the daytime images and applying GPS-based flow scaling. By using the two different sources for acquiring the pseudo-label, GPS-GLASS trains the nighttime semantic segmentation network without any annotation from nighttime images. The details of GPS-GLASS will be explained in the following subsections.

B. GPS-guided Learning Approach

1) *Pseudo-supervision using inter-domain matching*: Our key idea is to align P_d and P_n such that the aligned segmentation result can be used as the pseudo-label. To this end, inspired by SFNet [45], the correlation layer is adopted to compute the correlation of the image features between two different domains. Let $f^d = \{f_l^d, f_g^d\}$ be the set of the local and global features extracted from the semantic segmentation network for the input I_d . In case of PSPNet [5], which is our chosen architecture for semantic segmentation, f_l^d and f_g^d are extracted before and after passing through the PSP module of PSPNet, respectively, and have the same dimension of $H \times W \times D$. $f^n = \{f_l^n, f_g^n\}$ is extracted similarly from the semantic segmentation network for the input I_n . Then, the

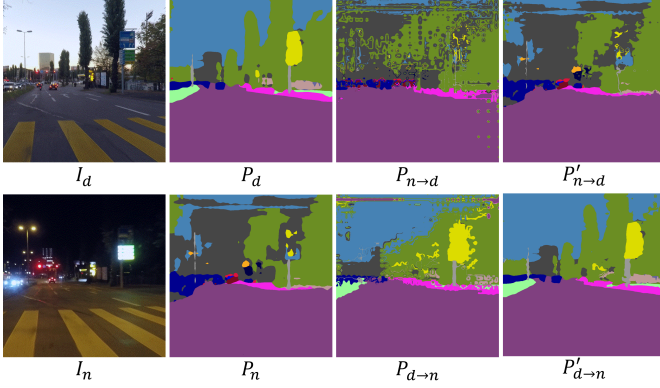


Fig. 3. Examples of the segmentation results and warped pseudo-labels obtained during training.

correlation layer computes the correlation between f^d and f^n as follows:

$$c_x(\mathbf{p}, \mathbf{q}) = \left(\frac{f_x^d(\mathbf{p})}{\|f_x^d(\mathbf{p})\|} \right)^\top \left(\frac{f_x^n(\mathbf{q})}{\|f_x^n(\mathbf{q})\|} \right), x \in \{l, g\}, \quad (1)$$

where \top is the transpose operator, $\|\cdot\|$ measures L2 norm, \mathbf{p} and \mathbf{q} represent 2D coordinates, and $f_x^d(\mathbf{p})$ and $f_x^n(\mathbf{p})$ are the D -dimensional vectors at \mathbf{p} and \mathbf{q} , respectively. We combine the correlation volumes obtained from the local and global features by $c = c_l \odot c_g$, where \odot represents element-wise multiplication. Instead of using the standard argmax function to obtain the correspondence from c , we use soft-argmax [46], [47] to allow backpropagation through the correlation layer as follows:

$$c'(\mathbf{p}, \mathbf{q}) = \frac{\exp(\alpha \cdot c(\mathbf{p}, \mathbf{q}))}{\sum_{\mathbf{q}' \in \mathbf{Q}} \exp(\alpha \cdot c(\mathbf{p}, \mathbf{q}'))}, \quad (2)$$

where \mathbf{Q} is the set of 2D positions in f^n , and α is the temperature parameter. Note that soft-argmax converges to argmax as α increases, but an excessively high value of α can lead to unstable gradient flow during training. The optical flow field from the daytime to nighttime $F_{d \rightarrow n}$ is obtained as

$$F_{d \rightarrow n}(\mathbf{p}) = \sum_{\mathbf{q} \in \mathbf{Q}} c'(\mathbf{p}, \mathbf{q}) \cdot \mathbf{q}. \quad (3)$$

The optical flow field from the nighttime to daytime $F_{n \rightarrow d}$ is obtained in a similar manner by switching \mathbf{p} and \mathbf{q} in Eqs. (1)-(3). Finally, the semantic segmentation map warped from nighttime to daytime, denoted as $P_{n \rightarrow d}$, is obtained using $F_{d \rightarrow n}$ and P_n by backward warping. Similarly, the semantic segmentation map warped from daytime to nighttime, denoted as $P_{d \rightarrow n}$, is obtained using $F_{n \rightarrow d}$ and P_d . Fig 3 shows some examples of $P_{n \rightarrow d}$ and $P_{d \rightarrow n}$. Although these warped predictions are imperfect, $P_{n \rightarrow d}$ ($P_{d \rightarrow n}$) is expected to be close to P_d (P_n). Therefore, we can use $P_{n \rightarrow d}$ and $P_{d \rightarrow n}$ for the nighttime semantic segmentation network training.

2) *Pseudo-supervision using intra-domain matching*: Due to the suboptimal performance of the relighting network, dense correspondence matching between daytime and nighttime is still challenging. Observing that most existing semantic image segmentation datasets [1], [2], [7] provide video frames, we

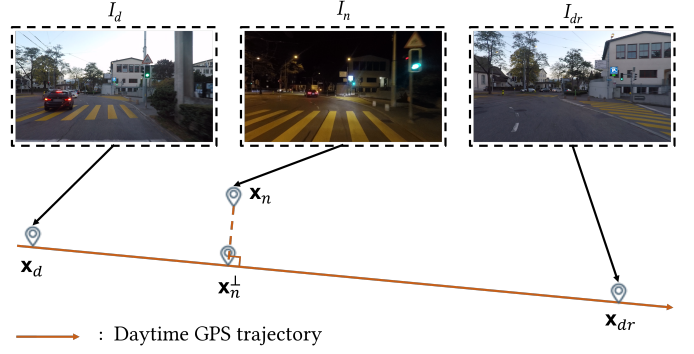


Fig. 4. Illustration of the nighttime, daytime, and daytime reference images with their corresponding GPS positions.

propose to use another daytime reference image, denoted as I_{dr} , for generating an additional pseudo-label. In the Dark Zurich dataset, I_n is the nearest nighttime image of I_d , but the neighboring frames of I_d along the forward and backward directions, denoted as I_d^+ and I_d^- , are also available. From the GPS positions of these images, we can determine I_{dr} as either I_d^+ or I_d^- .

Specifically, let \mathbf{x}_d , \mathbf{x}_d^+ , \mathbf{x}_d^- , and \mathbf{x}_n denote the GPS positions of I_d , I_d^+ , I_d^- , and I_n , respectively. Here, each GPS position is given as a 2D vector containing the latitude and longitude. Then, I_{dr} is determined as follows:

$$I_{dr} = \begin{cases} I_d^+, & \text{if } CS(\mathbf{x}_d - \mathbf{x}_n, \mathbf{x}_d^+ - \mathbf{x}_n) \\ & < CS(\mathbf{x}_d - \mathbf{x}_n, \mathbf{x}_d^- - \mathbf{x}_n), \\ I_d^-, & \text{otherwise,} \end{cases} \quad (4)$$

where CS measures the cosine similarity. In other words, as illustrated in Fig. 4, if I_n is located along the forward direction of I_d , I_d^+ is chosen as I_{dr} . Otherwise, I_d^- is chosen as I_{dr} .

Given I_d and I_{dr} , we obtain the optical flow field from the daytime to daytime reference, denoted as $F_{d \rightarrow dr}$, by following the same procedure of Eqs. (1)-(3) but with the features f^d and f^{dr} , where $f^{dr} = \{f_l^{dr}, f_g^{dr}\}$ is the feature extracted from I_{dr} . The optical flow field from the daytime reference to daytime $F_{dr \rightarrow d}$ is obtained similarly. For the generation of the pseudo-label for the nighttime semantic segmentation network training, another pair of the optical flow fields are obtained as $F'_{d \rightarrow n} = \lambda F_{d \rightarrow dr}$ and $F'_{n \rightarrow d} = \lambda F_{dr \rightarrow d}$. The scale factor λ is chosen as

$$\lambda = \frac{HD(\mathbf{x}_d, \mathbf{x}_n^\perp)}{HD(\mathbf{x}_d, \mathbf{x}_{dr})}, \quad (5)$$

where HD measures the Haversine distance of two positions [48], and \mathbf{x}_n^\perp represents the position projected onto the line joining \mathbf{x}_d and \mathbf{x}_{dr} , as illustrated in Fig. 4. Finally, the semantic segmentation map warped from nighttime to daytime, denoted as $P'_{n \rightarrow d}$, is obtained using $F'_{d \rightarrow n}$ and P_n by backward warping. Similarly, the semantic segmentation map warped from daytime to nighttime, denoted as $P'_{d \rightarrow n}$, is obtained using $F'_{n \rightarrow d}$ and P_d . Fig 3 shows some examples of $P'_{n \rightarrow d}$ and $P'_{d \rightarrow n}$. We now have four warped segmentation maps, i.e., $P_{n \rightarrow d}$, $P_{d \rightarrow n}$, $P'_{n \rightarrow d}$, and $P'_{d \rightarrow n}$, which are used for the nighttime semantic segmentation network training.

3) *Confidence map*: The first pair of the warped predictions, i.e., $P_{n \rightarrow d}$ and $P_{d \rightarrow n}$, can be inaccurate due to imperfect relighting and flow estimation. The second pair of the warped predictions, i.e., $P'_{n \rightarrow d}$ and $P'_{d \rightarrow n}$, can also be inaccurate because \mathbf{x}_n is generally not lying on the line joining \mathbf{x}_d and \mathbf{x}_{dr} , and thus the simple scaling by λ can lead to imprecise flow fields. Moreover, GPS positions are not always precise. We thus define a 2D confidence map such that only consistent predictions are used for pseudo-supervision. Specifically, the confidence map for the nighttime to daytime warping, denoted as $M_{n \rightarrow d}$, is defined as follows:

$$\mathbf{I}(\mathbf{p}) = \left\{ \mathbf{i} \mid \operatorname{argmax}(P_{n \rightarrow d}(\mathbf{p})) = \operatorname{argmax}(P'_{n \rightarrow d}(\mathbf{p} + \mathbf{i})) \right\}, \quad (6)$$

$$M_{n \rightarrow d}(\mathbf{p}) = \begin{cases} 1, & \text{if } \exists \mathbf{I}(\mathbf{p}) \in \Omega, \\ 0, & \text{otherwise,} \end{cases} \quad (7)$$

where Ω is a set of positions in the 3×3 kernel. $P_{n \rightarrow d}(\mathbf{p})$ extracts the C -dimensional vector at \mathbf{p} , where C is the number of semantic classes. The confidence map for the daytime to nighttime warping, denoted as $M_{d \rightarrow n}$, can be defined in a similar manner. These binary confidence maps are used when training the nighttime semantic network.

C. Objective Functions

We use five loss terms for GPS-GLASS: light loss L_{light} , semantic segmentation loss L_{seg} , adversarial loss L_{adv} , discriminator loss L_{dis} , and warping loss. Because we use the same loss functions defined in DANNet for the first four terms [10], we only detail the warping loss in this subsection.

We now have $P_{n \rightarrow d}$ and $P_{d \rightarrow n}$ and their confidence maps $M_{n \rightarrow d}$ and $M_{d \rightarrow n}$, which can be used to supervise the training of the nighttime semantic segmentation network. Note that $P'_{n \rightarrow d}$ and $P'_{d \rightarrow n}$ are integrated to $P_{n \rightarrow d}$ and $P_{d \rightarrow n}$ since only consistent predictions are used by the confidence maps. First, we use $P_{d \rightarrow n}$ for the pseudo-supervision of P_n . Specifically, the first warping loss term $L_{d \rightarrow n}$ is defined as follows:

$$H(P_{d \rightarrow n}(\mathbf{q}), P_n(\mathbf{q})) = \sum_{k \in \mathbb{C}} E_o(P_{d \rightarrow n}(\mathbf{q}; k)) \log P_n(\mathbf{q}; k), \quad (8)$$

$$L_{d \rightarrow n} = -\frac{1}{N_p \cdot C} \sum_{\mathbf{q} \in \mathbb{Q}^-} M_{d \rightarrow n}(\mathbf{q}) H(P_{d \rightarrow n}(\mathbf{q}), P_n(\mathbf{q})), \quad (9)$$

where H measures the cross entropy, E_o denotes the one-hot encoding [10], \mathbb{C} is a set of all semantic segmentation classes, N_p is the number of pixels. $P_n(\mathbf{q}; k)$ represents the probability of the k -th object class at the position \mathbf{q} of P_n . Note that the cross-entropy loss is measured only for the reliable prediction with $M_{d \rightarrow n}(\mathbf{q}) = 1$. Here, we define a set of ignore indexes, $\tilde{\mathbb{Q}}$, as follows:

$$\tilde{\mathbb{Q}} = \left\{ \mathbf{q} \mid \begin{array}{l} \operatorname{argmax}(P_n(\mathbf{q})) \in \mathbb{C}_{dyn}, \\ \operatorname{argmax}(P_n(\mathbf{q})) \neq \operatorname{argmax}(P_{d \rightarrow n}(\mathbf{q})) \end{array} \right\}, \quad (10)$$

where \mathbb{C}_{dyn} is a set of dynamic semantic classes, including cars, people, etc. Then, \mathbb{Q}^- in Eq. (10) is defined as $\mathbb{Q}^- = \mathbb{Q} \cap \tilde{\mathbb{Q}}^c$. We found this special handling is necessary to prevent undesirable pseudo-supervision of dynamic object classes.

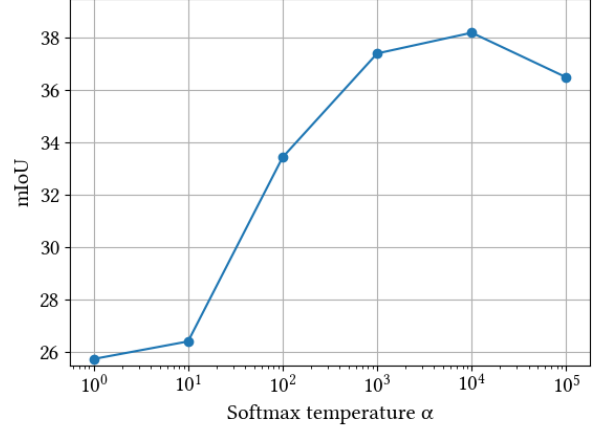


Fig. 5. Performance evaluation with different softmax temperature values on Dark Zurich-val.

The second warping loss $L_{n \rightarrow d}$ is defined as follows:

$$L_{n \rightarrow d} = -\frac{1}{N_p \cdot C} \sum_{\mathbf{p} \in \mathbb{P}^-} M_{n \rightarrow d}(\mathbf{p}) H(P_d(\mathbf{p}), P_{n \rightarrow d}(\mathbf{p})), \quad (11)$$

where \mathbb{P}^- is defined in a similar manner as \mathbb{Q}^- . In other words, P_d is used as the pseudo-supervision of $P_{n \rightarrow d}$ for the nighttime segmentation network training.

The objective functions for the target daytime and nighttime domains, L_{T_d} and L_{T_n} , and the source domain L_S are defined as:

$$L_{T_d} = \mu_1 L_{light} + \mu_2 L_{adv}, \quad (12)$$

$$L_{T_n} = \mu_1 L_{light} + L_{n \rightarrow d} + L_{d \rightarrow n} + \mu_2 L_{adv}, \quad (13)$$

$$L_S = \mu_1 L_{light} + \mu_3 L_{seg} + \mu_4 L_{dis}, \quad (14)$$

where μ_1 , μ_2 , μ_3 , and μ_4 are empirically chosen as 0.01, 0.01, 1, and 1, respectively. In every training iteration of GPS-GLASS, we sequentially optimize L_{T_d} , L_{T_n} , and L_S for daytime, nighttime, and source domains, respectively.

IV. EXPERIMENTAL RESULTS

A. Datasets

The **Cityscapes dataset** [1] includes 5,000 images taken in street scenes with pixel-level annotations for a total of 19 categories. The spatial resolution of the original images and annotations is $2,048 \times 1,024$. We used the training dataset of 2,975 images as the labeled source domain S in the GPS-GLASS training stage.

The **Dark Zurich dataset** [6] includes 2,416 nighttime images, 2,920 twilight images and 3,041 daytime images for training, which are all unlabeled with the size of $1,920 \times 1,080$. The images across different domains are coarsely paired according to the GPS distance-based nearest neighbor assignment. Consequently, most of these images share many image contents that are valuable for domain adaptation in semantic segmentation. Following the previous works [10], [11], we only used 2,416 day-night image pairs in the training

TABLE I

PERFORMANCE COMPARISON ON DARK ZURICH-TEST. THE BEST AND SECOND-BEST RESULTS ARE BOLDFACED AND UNDERLINED, RESPECTIVELY.

Method	road	sidewalk	building	wall	fence	pole	light	sign	vegetation	terrain	sky	person	rider	car	truck	bus	train	motorcycle	bicycle	mIoU
RefineNet	68.8	23.2	46.8	20.8	12.6	29.8	30.4	26.9	43.1	14.3	0.3	36.9	49.7	63.6	6.8	0.2	24.0	33.6	9.3	28.5
DeepLabV2	79.0	21.8	53.0	13.3	11.2	22.5	20.2	22.1	43.5	10.4	18.0	37.4	33.8	64.1	6.4	0.0	52.3	30.4	7.4	28.8
PSPNet	78.2	19.0	51.2	15.5	10.6	30.3	28.9	22.0	56.7	13.3	20.8	38.2	21.8	52.1	1.6	0.0	53.2	23.2	10.7	28.8
AdaptSegNet	86.1	44.2	55.1	22.2	4.8	21.1	5.6	16.7	37.2	8.4	1.2	35.9	26.7	68.2	45.1	0.0	50.1	33.9	15.6	30.4
ADVENT	85.8	37.9	55.5	27.7	14.5	23.1	14.0	21.1	32.1	8.7	2.0	39.9	16.6	64.0	13.8	0.0	58.8	28.5	20.7	29.7
BDL	85.3	41.1	61.9	32.7	17.4	20.6	11.4	21.3	29.4	8.9	1.1	37.4	22.1	63.2	28.2	0.0	47.7	39.4	15.7	30.8
DMAda	75.5	29.1	48.6	21.3	14.3	34.3	36.8	29.9	49.4	13.8	0.4	43.3	<u>50.2</u>	69.4	18.4	0.0	27.6	34.9	11.9	32.1
GCMA	81.7	46.9	58.8	22.0	20.0	41.2	40.5	41.6	64.8	31.0	32.1	53.5	<u>47.5</u>	75.5	39.2	0.0	49.6	30.7	21.0	42.0
MGCDa	80.3	49.3	66.2	7.8	11.0	41.4	38.9	<u>39.0</u>	64.1	18.0	55.8	<u>52.1</u>	53.5	<u>74.7</u>	66.0	0.0	37.5	29.1	22.7	42.5
DANNet	90.4	60.1	71.0	33.6	22.9	<u>30.6</u>	34.3	33.7	<u>70.5</u>	31.8	80.2	45.7	41.6	<u>67.4</u>	16.8	0.0	73.0	31.6	<u>22.9</u>	45.2
CDAda	90.5	60.6	67.9	<u>37.0</u>	19.3	42.9	36.4	35.3	66.9	24.4	79.8	45.4	42.9	70.8	<u>51.7</u>	0.0	29.7	27.7	26.2	45.0
DANIA	<u>91.5</u>	<u>62.7</u>	73.9	39.9	<u>25.7</u>	36.5	35.7	36.2	71.4	35.3	<u>82.2</u>	48.0	44.9	73.7	11.3	<u>0.1</u>	<u>64.3</u>	<u>36.7</u>	22.7	47.0
GPS-GLASS	91.6	63.1	<u>71.2</u>	34.7	26.7	<u>41.4</u>	<u>39.7</u>	38.4	68.6	<u>34.8</u>	83.7	41.3	40.8	69.6	21.5	0.0	63.5	32.1	19.4	<u>46.4</u>

TABLE II

PERFORMANCE COMPARISON ON DARK ZURICH-VAL AND NIGHTCITY+.

Method	mIoU	
	Dark Zurich-val	NightCity+
RefineNet	15.16	-
DeepLabV2	12.14	-
PSPNet	12.28	19.04
AdaptSegNet	20.19	-
GCMA	26.65	-
MGCDa	26.10	-
DANNet	36.76	29.93
CDAda	36.0	-
DANIA	38.14	28.92
GPS-GLASS	38.19	31.81

stage of GPS-GLASS as the unlabeled target domains, T_d and T_n . For the quantitative performance evaluation, the Dark Zurich dataset provides 50 finely annotated nighttime images (Dark Zurich-val), which are also used for our ablation study. Because the ground-truth segmentation labels of 151 images for testing (Dark Zurich-test) are not publicly available, the performance evaluation was conducted on the online evaluation website [49].

The **ACDC-night dataset** [50] is an extended version of the Dark Zurich dataset, including 1006 nighttime images (400, 106, and 500 images for training, validation, and test). The dataset also provides finely annotated nighttime images as the Dark Zurich dataset. The performance evaluation on the ACDC-night dataset was conducted on a test set using an online evaluation website [51].

The **NightCity+ dataset** [52] is an extended version of the NightCity dataset [53] that re-annotates incorrectly labeled regions of the validation set. The NightCity+ dataset provides 2998 and 1299 images for training and validation, respectively, which were taken from nighttime street scenes in various cities. We used the NightCity+ validation dataset only for the performance evaluation.

B. Implementation Details

We implemented GPS-GLASS using PyTorch. The training was performed with a single Nvidia Titan RTX GPU. Following [54] [54], we trained our network using the stochastic gradient descent optimizer with a momentum of 0.9 and a weight decay of 5×10^{-4} . We used Adam optimizer [55] for training the discriminators with β of 0.9 and 0.99. The initial learning rate of the generator and discriminators was set to 2.5×10^{-4} and then reduced to the power of 0.9 using the poly learning rate policy. For data augmentation, random cropping of the size 512×512 was applied with a scale factor between 0.5 and 1.0 for the Cityscapes dataset, and random cropping of the size 960×960 was applied with a scale factor between 0.9 and 1.1 for the Dark Zurich dataset. In addition, we applied random horizontal flips for training. We used PSPNet [5] as the segmentation network model, which has shown state-of-the-art performance in nighttime semantic segmentation. We pre-trained PSPNet on the Cityscapes dataset for 150K iterations using L_{seg} . Then, we set the batch size to 2 and trained the model for 100K iterations.

We found that careful selection of the temperature value α in Eq. (2) is important for correspondence matching. The performance evaluation on Dark Zurich-val for GPS-GLASSES trained with different α values is shown in Fig. 5. From this grid search of α , we chose $\alpha = 10^4$ in our experiments.

C. Comparison with State-of-the-art Methods

1) *Comparison on Dark Zurich*: We compared GPS-GLASS with several state-of-the-art domain adaptation-based nighttime semantic segmentation methods, including CDAda [11], DANNet [10], DANIA [30], MGCDa [7], GCMA [6], and DMAda [3]. For the comparison with the other techniques, BDL, AdaptSegNet, ADVENT [56]–[58] were also evaluated, where they were trained to adapt from Cityscapes to Dark Zurich-N. We report the mean intersection over union (mIoU) as the evaluation metric. Table I reports the mIoU results on Dark Zurich-test. All of these compared methods used the common ResNet-101 [59] as a backbone. We

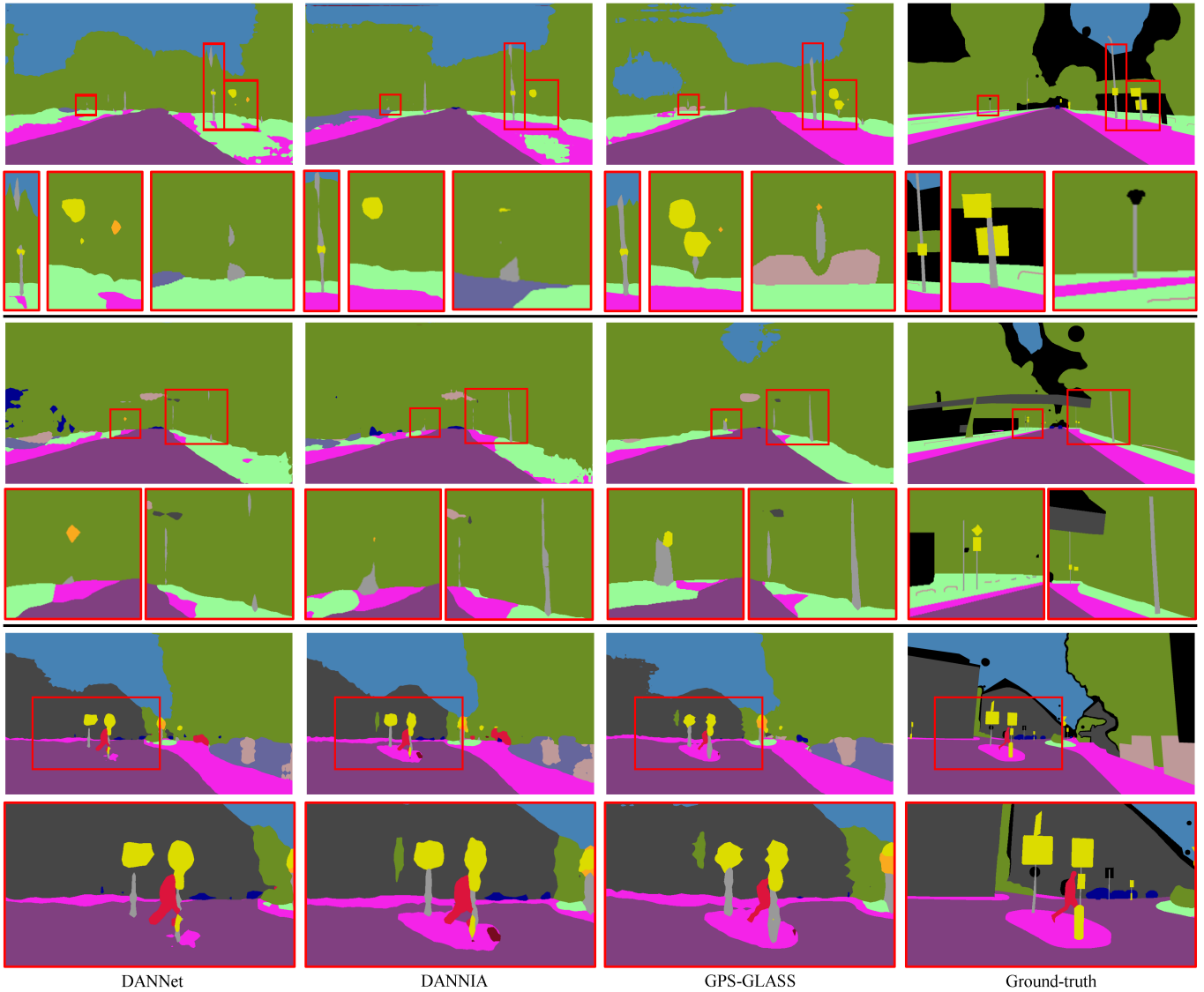


Fig. 6. More results of our proposed GPS-GLASS, DANNet, and DANIA for visual comparison. The results in the red boxes are zoomed in for better visualization. Note that small object classes, such as pole and lights, are more precisely segmented by GPS-GLASS compared to DANNet and DANIA. In addition, object classes sharing similar features, such as road and sidewalk, are well separated by GPS-GLASS.

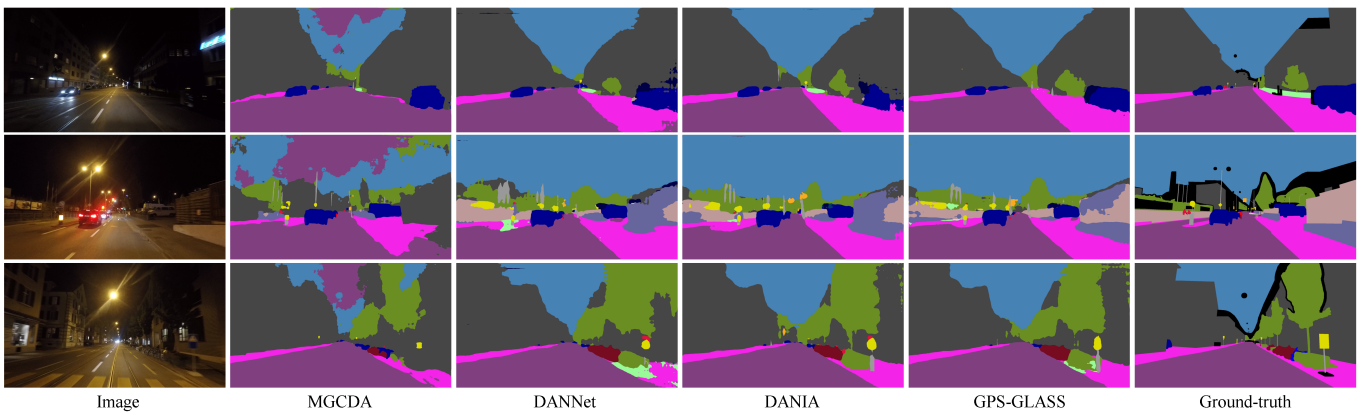


Fig. 7. Visual comparison of our GPS-GLASS with other state-of-the-art methods on Dark Zurich-val.

TABLE III
PERFORMANCE COMPARISON ON ACDC-NIGHT. THE BEST AND SECOND-BEST RESULTS ARE BOLDFACED AND UNDERLINED, RESPECTIVELY.

Method	road	sidewalk	building	wall	fence	pole	light	sign	vegetation	terrain	sky	person	rider	car	truck	bus	train	motorcycle	bicycle	mIoU
RefineNet	66.8	24.0	50.3	16.9	11.6	26.4	34.2	25.5	44.2	21.6	0.1	40.8	24.8	57.4	6.8	37.3	20.5	24.0	19.1	29.1
DeepLabV2	77.0	22.9	56.3	13.5	9.2	23.8	22.9	25.6	41.4	16.1	2.9	44.2	17.5	64.1	11.9	34.5	42.4	22.7	22.7	30.1
PSPNet	75.5	16.3	47.3	14.5	10.4	23.2	29.0	22.8	40.5	10.8	12.0	39.2	15.3	44.3	2.6	23.0	37.5	13.8	27.9	26.6
DMAda	74.7	29.5	49.4	17.1	12.6	31.0	38.2	30.0	48.0	22.8	0.2	47.0	25.4	63.8	12.8	46.1	23.1	24.7	24.6	32.7
GCMA	78.6	45.9	58.5	17.7	18.6	<u>37.5</u>	43.6	43.5	58.7	39.2	22.5	57.9	29.9	72.1	21.5	<u>56.3</u>	41.8	35.7	35.4	42.9
MGCDA	74.5	52.5	69.4	7.7	10.8	38.4	<u>40.2</u>	<u>43.3</u>	61.5	36.3	37.6	<u>55.3</u>	25.6	<u>71.2</u>	10.9	46.4	32.6	27.3	33.8	40.8
DANNet	90.7	<u>61.2</u>	75.6	35.9	28.8	26.6	31.4	30.6	70.8	<u>39.4</u>	78.7	49.9	28.8	65.9	<u>24.7</u>	44.1	61.1	25.9	34.5	47.6
DANIA	<u>91.0</u>	<u>60.9</u>	77.7	40.3	30.7	34.3	37.9	34.5	<u>70.0</u>	37.2	<u>79.6</u>	45.7	32.6	66.4	11.1	37.0	<u>60.7</u>	<u>32.6</u>	37.9	<u>48.3</u>
GPS-GLASS	91.8	65.0	<u>76.4</u>	<u>38.1</u>	<u>30.0</u>	35.8	38.5	37.6	69.2	41.4	79.8	45.8	<u>31.2</u>	69.6	38.0	59.9	45.7	24.9	<u>37.2</u>	50.3

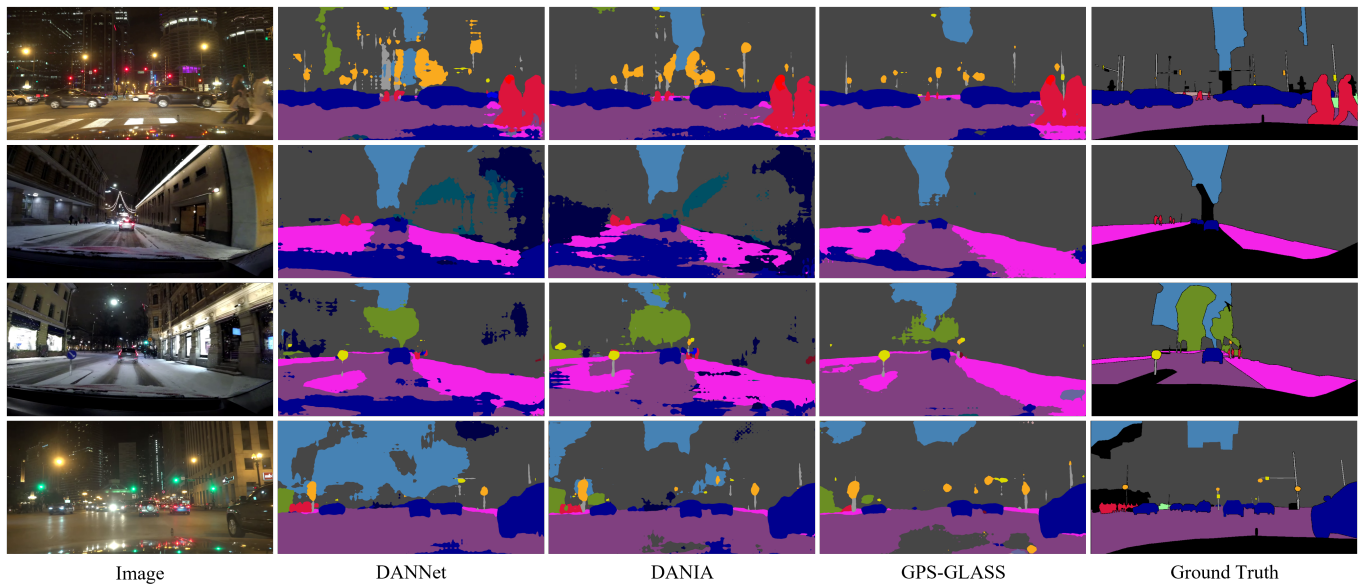


Fig. 8. Visual comparison of our GPS-GLASS with other state-of-art methods on NightCity+.

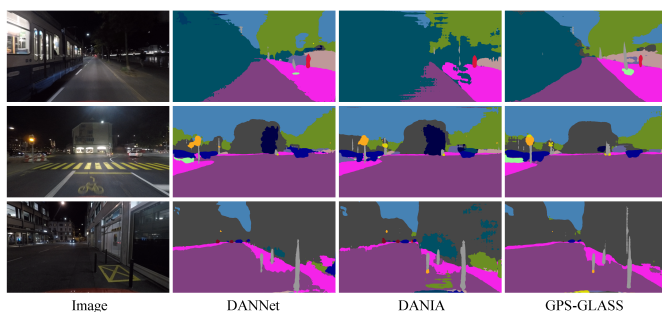


Fig. 9. Visual comparison of our GPS-GLASS with other state-of-art methods on ACDC-night.

used DANNet and DANIA with PSPNet for a fair comparison with our GPS-GLASS.

GPS-GLASS achieved a 1.2% performance improvement in terms of the mIoU over the baseline method, DANNet, and showed the second-best performance. Note that GPS-GLASS does not increase the number of network parameters or pro-

cessing time compared to DANNet because the same architecture of PSPNet is used in the inference stage. The performance improvements are significant in several categories, such as road, sidewalk, building, and terrain, which are difficult to identify in nighttime scenes. Meanwhile, due to pixel-level aligned pseudo-supervision, improvements are also noticeable in small-scale classes such as fences, poles, and lights, as shown in Fig. 6. Consistent results were obtained from Dark Zurich-val as shown in Table II. These results indicate that our approach effectively performed the domain adaptation from the daytime to nighttime. Fig. 7 shows several results for visual comparison. More frame-by-frame comparisons are provided on our project page.

2) *Generalization Ability*: To show the generalization ability of our proposed method, we tested our model trained on Dark Zurich to ACDC-night and NightCity+. As shown in Table III, GPS-GLASS achieved a 2.0% performance improvement in terms of the mIoU over the second-best method, DANIA. Note that ACDC-night is an extended version of Dark Zurich, including more images with difficult object classes to be segmented. Due to the use of pixel-level aligned pseudo-

TABLE IV
ABLATION STUDY ON SEVERAL MODEL VARIANTS OF OUR METHOD ON DARK ZURICH-VAL.

	avg	max	confidence	inter	intra	$L_{n \rightarrow d}$	$L_{d \rightarrow n}$	local feature	global feature	static loss	mIoU	Gain
w/o pseudo-supervision											24.68	
DANNet										✓	36.76	+12.08
inter-intra mixing	✓			✓	✓	✓	✓	✓	✓		35.92	+11.24
		✓		✓	✓	✓	✓	✓	✓		35.70	+11.02
matching domain			✓	✓		✓	✓	✓	✓		34.86	+10.18
			✓		✓	✓	✓	✓	✓		36.21	+11.53
w/o one warping loss			✓	✓	✓	✓		✓	✓		33.90	+9.22
			✓	✓	✓		✓	✓	✓		36.06	+11.38
w/o global/local feature			✓	✓	✓	✓	✓	✓			36.62	+11.94
			✓	✓	✓	✓	✓		✓		36.67	+11.99
GPS-GLASS			✓	✓	✓	✓	✓	✓	✓		38.19	+13.51

supervision in GPS-GLASS, the performance improvements are especially noticeable in dynamic classes such as car, bus, and truck, which are important object classes for autonomous driving. Moreover, the performance evaluation on NightCity+ demonstrates that GPS-GLASS outperforms the other compared methods by a large margin, as shown in Table II. These results demonstrate that the proposed GPS-GLASS trained on Dark Zurich generalizes well to other challenging images. Figs. 9 and 8 show several results for visual comparison on ACDC-night and NightCity+, respectively, and more results can be found in our project page.

D. Ablation Study

In order to demonstrate the effectiveness of individual components of GPS-GLASS, several modified models of GPS-GLASS were trained, and the best performances in Dark Zurich-val are reported in Table IV. GPS-GLASS without any pseudo-supervision serves a naive baseline, which leads to the lowest mIoU of 24.68. Due to the static loss [10], DANNet achieved a 12.08% mIoU increase compared to the baseline. We applied other inter-intra pseudo-label mixing methods: taking the average of two pseudo-labels or taking the label with the higher probability for each pixel. For Dark Zurich-val, these two methods, denoted as avg and max in Table IV, increased the mIoU by 11.24% and 11.02%, respectively, which are worse than the performance improvement obtained using the confidence map (13.51%). Both warping loss terms, $L_{n \rightarrow d}$ and $L_{d \rightarrow n}$, were found to be essential compared to their single-use. In addition, because we obtained the integrated correlation volume by element-wise multiplication of the correlation volumes from the local and global features, we evaluated the performance obtained without using the local or global feature. The use of both features resulted in 1.57% or 1.52% higher mIoU compared to the single-use of the local or global feature, respectively. Last, because GPS-GLASS obtains pseudo-supervision from both intra-matching and inter-matching, we evaluated the performance without applying intra-matching or inter-matching and obtained 3.33% or 1.98% lower mIoU compared to GPS-GLASS, respectively.

V. CONCLUSIONS

In this paper, we proposed GPS-GLASS, a novel training methodology for nighttime semantic segmentation based on unlabeled daytime-nighttime image pairs and their GPS data. GPS-GLASS obtains pixel-level aligned pseudo-supervision through bidirectional correspondence matching between the daytime and nighttime. To address the difficulty of correspondence matching between different domains, GPS-GLASS also acquires another pseudo-supervision through correspondence matching in the same daytime domain using the GPS data. The confidence map is used to exclude pseudo-supervision of less reliable predictions. Our GPS-GLASS does not increase the number of network parameters or inference time compared to the adopted baseline model. Experimental results on the Dark Zurich, ACDC-night, and NightCity+ datasets demonstrate the effectiveness of the proposed method.

REFERENCES

- [1] M. Cordts, M. Omran, S. Ramos, T. Rehfeld, M. Enzweiler, R. Benenson, U. Franke, S. Roth, and B. Schiele, "The cityscapes dataset for semantic urban scene understanding," in *Proceedings of the IEEE/CVF Conference on Computer Vision and Pattern Recognition*, 2016, pp. 3213–3223.
- [2] A. Geiger, P. Lenz, C. Stiller, and R. Urtasun, "Vision meets robotics: The KITTI dataset," *The International Journal of Robotics Research*, 2013.
- [3] D. Dai and L. Van Gool, "Dark model adaptation: Semantic image segmentation from daytime to nighttime," in *Proceedings of the International Conference on Intelligent Transportation Systems*, 2018, pp. 3819–3824.
- [4] F. Yu, H. Chen, X. Wang, W. Xian, Y. Chen, F. Liu, V. Madhavan, and T. Darrell, "BDD100K: A diverse driving dataset for heterogeneous multitask learning," in *Proceedings of the IEEE/CVF Conference on Computer Vision and Pattern Recognition*, 2020, pp. 2636–2645.
- [5] H. Zhao, J. Shi, X. Qi, X. Wang, and J. Jia, "Pyramid scene parsing network," in *Proceedings of the IEEE/CVF Conference on Computer Vision and Pattern Recognition*, 2017, pp. 2881–2890.
- [6] C. Sakaridis, D. Dai, and L. V. Gool, "Guided curriculum model adaptation and uncertainty-aware evaluation for semantic nighttime image segmentation," in *Proceedings of the IEEE/CVF International Conference on Computer Vision*, 2019, pp. 7374–7383.
- [7] C. Sakaridis, D. Dai, and L. Van Gool, "Map-guided curriculum domain adaptation and uncertainty-aware evaluation for semantic nighttime image segmentation," *IEEE Trans. Pattern Anal. Mach. Intell.*, 2020.
- [8] E. Romera, L. M. Bergasa, K. Yang, J. M. Alvarez, and R. Barea, "Bridging the day and night domain gap for semantic segmentation," in *Proceedings of the IEEE Intelligent Vehicles Symposium (IV)*, 2019, pp. 1312–1318.

- [9] L. Sun, K. Wang, K. Yang, and K. Xiang, "See clearer at night: towards robust nighttime semantic segmentation through day-night image conversion," in *Proceedings of the Artificial Intelligence and Machine Learning in Defense Applications*, vol. 11169, 2019, p. 111690A.
- [10] X. Wu, Z. Wu, H. Guo, L. Ju, and S. Wang, "Dannet: A one-stage domain adaptation network for unsupervised nighttime semantic segmentation," in *Proceedings of the IEEE/CVF Conference on Computer Vision and Pattern Recognition*, 2021, pp. 15769–15778.
- [11] Q. Xu, Y. Ma, J. Wu, C. Long, and X. Huang, "CDAda: A curriculum domain adaptation for nighttime semantic segmentation," in *Proceedings of the IEEE/CVF International Conference on Computer Vision*, 2021, pp. 2962–2971.
- [12] S. R. Richter, V. Vineet, S. Roth, and V. Koltun, "Playing for data: Ground truth from computer games," in *Proceedings of the European Conference on Computer Vision*. Springer, 2016, pp. 102–118.
- [13] A. Zheng, M. Wang, C. Li, J. Tang, and B. Luo, "Entropy guided adversarial domain adaptation for aerial image semantic segmentation," *IEEE Trans. Geosci. Remote Sens.*, 2022.
- [14] T. Chen, S.-H. Wang, Q. Wang, Z. Zhang, G.-S. Xie, and Z. Tang, "Enhanced feature alignment for unsupervised domain adaptation of semantic segmentation," *IEEE Trans. Multimedia*, 2022.
- [15] Y. Ganin, E. Ustinova, H. Ajakan, P. Germain, H. Larochelle, F. Laviolette, M. Marchand, and V. Lempitsky, "Domain-adversarial training of neural networks," *Journal of Machine Learning Research*, 2016.
- [16] J. Hoffman, D. Wang, F. Yu, and T. Darrell, "Fcns in the wild: Pixel-level adversarial and constraint-based adaptation," *arXiv preprint arXiv:1612.02649*, 2016.
- [17] L. Du, J. Tan, H. Yang, J. Feng, X. Xue, Q. Zheng, X. Ye, and X. Zhang, "SSF-DAN: Separated semantic feature based domain adaptation network for semantic segmentation," in *Proceedings of the IEEE/CVF International Conference on Computer Vision*, 2019, pp. 982–991.
- [18] Y.-H. Tsai, K. Sohn, S. Schuler, and M. Chandraker, "Domain adaptation for structured output via discriminative patch representations," in *Proceedings of the IEEE/CVF International Conference on Computer Vision*, 2019, pp. 1456–1465.
- [19] J. Choi, T. Kim, and C. Kim, "Self-ensembling with gan-based data augmentation for domain adaptation in semantic segmentation," in *Proceedings of the IEEE/CVF International Conference on Computer Vision*, 2019, pp. 6830–6840.
- [20] J. Hoffman, E. Tzeng, T. Park, J.-Y. Zhu, P. Isola, K. Saenko, A. Efros, and T. Darrell, "CycADA: Cycle-consistent adversarial domain adaptation," in *Proceedings of the International Conference on Machine Learning*, 2018, pp. 1989–1998.
- [21] Z. Wu, X. Han, Y.-L. Lin, M. G. Uzumbas, T. Goldstein, S. N. Lim, and L. S. Davis, "DCAN: Dual channel-wise alignment networks for unsupervised scene adaptation," in *Proceedings of the European Conference on Computer Vision*, 2018, pp. 518–534.
- [22] S. Lee, J. Hyun, H. Seong, and E. Kim, "Unsupervised domain adaptation for semantic segmentation by content transfer," in *Proceedings of the AAAI Conference on Artificial Intelligence*, 2021, pp. 8306–831.
- [23] Y. Yang and S. Soatto, "FDA: Fourier domain adaptation for semantic segmentation," in *Proceedings of the IEEE/CVF Conference on Computer Vision and Pattern Recognition*, 2020, pp. 4085–4095.
- [24] Y. Zhang, Z. Qiu, T. Yao, D. Liu, and T. Mei, "Fully convolutional adaptation networks for semantic segmentation," in *Proceedings of the IEEE/CVF Conference on Computer Vision and Pattern Recognition*, 2018, pp. 6810–6818.
- [25] D. Feng, C. Haase-Schütz, L. Rosenbaum, H. Hertlein, C. Glaeser, F. Timm, W. Wiesbeck, and K. Dietmayer, "Deep multi-modal object detection and semantic segmentation for autonomous driving: datasets, methods, and challenges," *IEEE Trans. Intell. Transp. Syst.*, 2020.
- [26] Y. Chen, W. Li, and L. Van Gool, "ROAD: Reality oriented adaptation for semantic segmentation of urban scenes," in *Proceedings of the IEEE/CVF Conference on Computer Vision and Pattern Recognition*, 2018, pp. 7892–7901.
- [27] S. Jeong, Y. Kim, E. Lee, and K. Sohn, "Memory-guided unsupervised image-to-image translation," in *Proceedings of the IEEE/CVF Conference on Computer Vision and Pattern Recognition*, 2021, pp. 6558–6567.
- [28] L. Jiang, C. Zhang, M. Huang, C. Liu, J. Shi, and C. C. Loy, "TSIT: A simple and versatile framework for image-to-image translation," in *Proceedings of the European Conference on Computer Vision*, 2020, pp. 206–222.
- [29] M.-Y. Liu, T. Breuel, and J. Kautz, "Unsupervised image-to-image translation networks," in *Proceedings of the Neural Information Processing Systems*, 2017, pp. 700–708.
- [30] X. Wu, Z. Wu, L. Ju, and S. Wang, "A one-stage domain adaptation network with image alignment for unsupervised nighttime semantic segmentation," *IEEE Trans. Pattern Anal. Mach. Intell.*, 2021.
- [31] P. Hu, G. Wang, and Y.-P. Tan, "Recurrent spatial pyramid cnn for optical flow estimation," *IEEE Trans. Multimedia*, 2018.
- [32] C. Zhang, Z. Zhou, Z. Chen, W. Hu, M. Li, and S. Jiang, "Self-attention-based multiscale feature learning optical flow with occlusion feature map prediction," *IEEE Trans. Multimedia*, 2021.
- [33] A. Dosovitskiy, P. Fischer, E. Ilg, P. Hausser, C. Hazirbas, V. Golkov, P. Van Der Smagt, D. Cremers, and T. Brox, "FlowNet: Learning optical flow with convolutional networks," in *Proceedings of the IEEE/CVF International Conference on Computer Vision*, 2015, pp. 2758–2766.
- [34] E. Ilg, N. Mayer, T. Saikia, M. Keuper, A. Dosovitskiy, and T. Brox, "FlowNet 2.0: Evolution of optical flow estimation with deep networks," in *Proceedings of the IEEE/CVF Conference on Computer Vision and Pattern Recognition*, 2017, pp. 2462–2470.
- [35] A. Ranjan and M. J. Black, "Optical flow estimation using a spatial pyramid network," in *Proceedings of the IEEE/CVF Conference on Computer Vision and Pattern Recognition*, 2017, pp. 4161–4170.
- [36] D. Sun, X. Yang, M.-Y. Liu, and J. Kautz, "Pwc-net: Cnns for optical flow using pyramid, warping, and cost volume," in *Proceedings of the IEEE/CVF Conference on Computer Vision and Pattern Recognition*, 2018, pp. 8934–8943.
- [37] Z. Teed and J. Deng, "Raft: Recurrent all-pairs field transforms for optical flow," in *Proceedings of the European Conference on Computer Vision*, 2020, pp. 402–419.
- [38] A. Vaswani, N. Shazeer, N. Parmar, J. Uszkoreit, L. Jones, A. N. Gomez, L. Kaiser, and I. Polosukhin, "Attention is all you need," in *Proceedings of the Advances in Neural Information Processing Systems*, 2017, pp. 5998–6008.
- [39] S. Jiang, D. Campbell, Y. Lu, H. Li, and R. Hartley, "Learning to estimate hidden motions with global motion aggregation," *arXiv preprint arXiv:2104.02409*, 2021.
- [40] H. Xu, J. Yang, J. Cai, J. Zhang, and X. Tong, "High-resolution optical flow from 1d attention and correlation," in *Proceedings of the IEEE/CVF International Conference on Computer Vision*, 2021, pp. 10498–10507.
- [41] H. Xu, J. Zhang, J. Cai, H. Rezatofighi, and D. Tao, "GMFlow: Learning optical flow via global matching," *arXiv preprint arXiv:2111.13680*, 2021.
- [42] H. Zhou, J. Ma, C. C. Tan, Y. Zhang, and H. Ling, "Cross-weather image alignment via latent generative model with intensity consistency," *IEEE Trans. Image Process.*, 2020.
- [43] P. Zhang, B. Zhang, D. Chen, L. Yuan, and F. Wen, "Cross-domain correspondence learning for exemplar-based image translation," in *Proceedings of the IEEE/CVF Conference on Computer Vision and Pattern Recognition*, 2020, pp. 5143–5153.
- [44] J. Lee, D. Kim, W. Lee, J. Ponce, and B. Ham, "Learning semantic correspondence exploiting an object-level prior," *IEEE Trans. Pattern Anal. Mach. Intell.*, 2020.
- [45] J. Lee, D. Kim, J. Ponce, and B. Ham, "SFNet: Learning object-aware semantic correspondence," in *Proceedings of the IEEE/CVF Conference on Computer Vision and Pattern Recognition*, 2019, pp. 2278–2287.
- [46] S. Honari, P. Molchanov, S. Tyree, P. Vincent, C. Pal, and J. Kautz, "Improving landmark localization with semi-supervised learning," in *Proceedings of the IEEE/CVF Conference on Computer Vision and Pattern Recognition*, 2018, pp. 1546–1555.
- [47] A. Kendall, H. Martirosyan, S. Dasgupta, P. Henry, R. Kennedy, A. Bachrach, and A. Bry, "End-to-end learning of geometry and context for deep stereo regression," in *Proceedings of the IEEE/CVF International Conference on Computer Vision*, 2017, pp. 66–75.
- [48] J. Inman, *Navigation and nautical astronomy, for the use of British seamen*. F. & J. Rivington, 1849.
- [49] C. Sakaridis, "UIoU Dark Zurich at Vision for All Seasons Workshop, CVPR 2020," <https://competitions.codalab.org/competitions/23553>, Feb 2020.
- [50] C. Sakaridis, D. Dai, and L. Van Gool, "ACDC: The adverse conditions dataset with correspondences for semantic driving scene understanding," in *Proceedings of the IEEE/CVF International Conference on Computer Vision*, 2021, pp. 10765–10775.
- [51] C. Sakaridis, "ACDC website," <https://acdc.vision.ee.ethz.ch/>, Feb. 2022.
- [52] X. Deng, P. Wang, X. Lian, and S. Newsam, "NightLab: A dual-level architecture with hardness detection for segmentation at night," in *Proceedings of the IEEE/CVF Conference on Computer Vision and Pattern Recognition*, 2022, pp. 16938–16948.
- [53] X. Tan, K. Xu, Y. Cao, Y. Zhang, L. Ma, and R. W. Lau, "Night-time scene parsing with a large real dataset," *IEEE Trans. Image Process.*, 2021.

- [54] L.-C. Chen, G. Papandreou, I. Kokkinos, K. Murphy, and A. L. Yuille, "Deeplab: Semantic image segmentation with deep convolutional nets, atrous convolution, and fully connected crfs," *IEEE Trans. Pattern Anal. Mach. Intell.*, 2017.
- [55] D. P. Kingma and J. Ba, "Adam: A method for stochastic optimization," in *Proceedings of International Conference on Learning Representations*, 2015.
- [56] Y.-H. Tsai, W.-C. Hung, S. Schulter, K. Sohn, M.-H. Yang, and M. Chandraker, "Learning to adapt structured output space for semantic segmentation," in *Proceedings of the IEEE/CVF Conference on Computer Vision and Pattern Recognition*, 2018, pp. 7472–7481.
- [57] T.-H. Vu, H. Jain, M. Bucher, M. Cord, and P. Pérez, "ADVENT: Adversarial entropy minimization for domain adaptation in semantic segmentation," in *Proceedings of the IEEE/CVF Conference on Computer Vision and Pattern Recognition*, 2019, pp. 2517–2526.
- [58] Y. Li, L. Yuan, and N. Vasconcelos, "Bidirectional learning for domain adaptation of semantic segmentation," in *Proceedings of the IEEE/CVF Conference on Computer Vision and Pattern Recognition*, 2019, pp. 6936–6945.
- [59] K. He, X. Zhang, S. Ren, and J. Sun, "Deep residual learning for image recognition," in *Proceedings of the IEEE/CVF Conference on Computer Vision and Pattern Recognition*, 2016, pp. 770–778.